Morphometric Risk Factors for Drusenoid Pigment Epithelium Detachment Collapse and Retinal Pigment Epithelium Atrophy Expansion

Matteo Menean,[1,2] Aurelio Apuzzo,[1,2] Ugo Introini,[1,2] Francesco Bandello,[1,2] and Maria Vittoria Cicinelli[1,2]

[1]School of Medicine, Vita-Salute San Raffaele University, Milan, Italy
[2]Department of Ophthalmology, IRCCS San Raffaele Scientific Institute, Milan, Italy

Correspondence: Maria Vittoria Cicinelli, FEBO, Department of Ophthalmology, IRCCS San Raffaele Scientific Institute, Via Olgettina 60, Milan 20132, Italy; cicinelli.mariavittoria@hsr.it.

Received: June 28, 2023
Accepted: November 30, 2023
Published: December 27, 2023

Citation: Menean M, Apuzzo A, Introini U, Bandello F, Cicinelli MV. Morphometric risk factors for drusenoid pigment epithelium detachment collapse and retinal pigment epithelium atrophy expansion. *Invest Ophthalmol Vis Sci.* 2023;64(15):38. https://doi.org/10.1167/iovs.64.15.38

Purpose. The purpose of this study was to investigate factors associated with drusenoid pigment epithelium detachment (dPED) growth rate, incidence of dPED collapse, and retinal pigment epithelium (RPE) atrophy enlargement rate following dPED collapse and their impact on visual acuity (VA).

Methods. This was a retrospective longitudinal study on 44 eyes. Serial spectral-domain optical coherence tomography (SD-OCT) and fundus autofluorescence (AF) imaging were performed. Qualitative features and quantitative dPED-related metrics were assessed. The surface-to-volume ratio (S/V) was computed to evaluate dPED shape irregularity. AF imaging was utilized to measure RPE atrophy area in eyes experiencing dPED collapse. Regression models were used to analyze associations among VA, dPED growth rate, and RPE atrophy enlargement rate. Cox regression was used to identify risk factors for dPED collapse.

Results. Significant correlations were observed between dPED area, surface, and volume ($P < 0.05$ for all pairs). The dPED metrics were inversely correlated with the S/V. Incidence of dPED collapse was 22 per 100 eye-years over a mean follow-up of 59 ± 41 months. Eyes experiencing collapsed dPED had worse baseline VA ($P < 0.001$). RPE hypertransmission (hazard ratio [HR] = 3.68, $P = 0.004$) and hyper-reflective foci (HR = 3.45, $P = 0.02$) were risk factors for dPED collapse; a higher S/V ratio was protective (HR = 0.78, $P = 0.03$). A faster rate of RPE atrophy enlargement was associated with a faster rate of dPED volume increase ($r = 0.47$, $P = 0.02$) and worse VA over time ($P = 0.02$).

Conclusions. Risk stratification in patients with dPED can be aided by identifying risk factors for dPED collapse. Identifying factors associated with RPE atrophy enlargement may have implications for treatment decision making.

Keywords: drusenoid pigment epithelium detachment (dPED), intermediate age-related macular degeneration (iAMD), visual acuity (VA), retinal pigment epithelium (RPE) atrophy

Drusenoid pigment epithelial detachments (dPED) occur when drusenoid material accumulates between the basal lamina (BL) of the retinal pigment epithelium (RPE) and the inner collagenous layer of Bruch's membrane (BrM).[1] These detachments exhibit a characteristic dome-shaped appearance and are typically hyper-reflective on spectral-domain optical coherence tomography (SD-OCT).

The prevalence of dPED is estimated to be approximately 8%, and it is considered a diagnostic criterion for intermediate age-related macular degeneration (iAMD).[2–4] Patients with dPED often experience worse vision compared to those without dPED and have an increased risk of progressing to late AMD.[2–4] The life cycle of dPED involves a slow phase of volume growth, followed by rapid collapse and re-absorption of the drusenoid material,[5,6] which can ultimately lead to the development of RPE atrophy or choroidal neovascularization (CNV).[4]

The size of dPED, its rate of growth, and the likelihood of progression to RPE atrophy can vary significantly among patients with iAMD.[7] SD-OCT has identified several risk factors for late AMD in eyes with dPED, including intraretinal hyper-reflective foci (HRF), defects in photoreceptors and RPE, and acquired vitelliform lesions (AVLs).[8,9] Additionally, morphometric parameters of dPED, such as maximum height, total volume, and largest width, have been found to play a significant role in the development of RPE atrophy.[6,10] However, it remains unclear whether the combination of these metrics and their dynamic changes contribute to the likelihood of dPED re-absorption and the dynamics of RPE atrophy growth.

With the availability of new treatments for halting the progression of late AMD,[11,12] it is crucial to identify biomarkers that can predict the risk of progression to RPE atrophy and faster RPE atrophy expansion. Therefore, this study aimed to investigate the associations between the dynamic properties of dPED and the risk of dPED collapse and RPE atrophy development. Additionally, we aimed to explore the factors associated with the rate of RPE atrophy expansion following dPED collapse. Understanding these dynamic changes in dPED may have important implications for predicting long-term visual and morphological outcomes and could serve as prognostic factors.

Methods

Study Design and Participants

This longitudinal, retrospective study included patients with iAMD who were seen at the San Raffaele Scientific Institute in Milan, Italy, between April 2011 and March 2023. The study was conducted in accordance with the principles of the Declaration of Helsinki, and written informed consent was waived by the local institutional review board (IRB).

Patients aged 50 years and older diagnosed with iAMD were identified from the outpatient clinic. Only patients with foveal dPED measuring at least 350 µm[2,13] in diameter were consecutively enrolled in the study. The baseline visit was the first recorded visit in the electronic medical chart, and all subsequent visits were reviewed. Eyes with CNV, serous, hemorrhagic, or fibrovascular PED, other retinal comorbidities, or opacities of the optic media affecting imaging quality were excluded from the analysis. Patients receiving any ocular treatment (injections, laser, or photobiomodulation) were also excluded. There was no specified minimum follow-up duration.

Demographics and ophthalmic history data were collected at the first visit. At each encounter, refracted visual acuity (VA) was performed. All eyes underwent blue-light fundus autofluorescence (BAF) of the central 30 degrees and a horizontal 19-raster SD-OCT scan covering an area of 20 × 15 degrees using eye tracking, an enhanced depth imaging modality, and a follow-up mode (Spectralis HRA+OCT; Heidelberg Engineering, Heidelberg, Germany). Additional imaging was performed at the discretion of the physician.

SD-OCT scans were evaluated at baseline and the visit immediately prior to dPED collapse. The dPED collapse was defined as a reduction of 50% or more in its height.[14] For eyes that did not experience dPED collapse, the analysis was repeated at the last available visit. SD-OCT scans were analyzed by two trained ophthalmology residents (authors M.M. and A.A.) masked regarding the final event under the supervision of a retina specialist (author M.V.C.). A two-way mixed-effect (i.e. the selected raters were the only raters of interest), average measurement model was used to calculate the intraclass correlation coefficient (ICC) as a measure of agreement (Supplementary Table S1).[15]

Qualitative SD-OCT Measurements

The SD-OCT scans were assessed for the presence of subretinal fluid, AVL, intraretinal HRF, and RPE hypertransmission, and reticular pseudodrusen. AVL was defined as subretinal material hyper-reflective on SD-OCT and hyperautofluorescent on BAF. HRF were defined as discrete, well-circumscribed, punctate lesions with equal or greater reflectivity than RPE. The RPE hypertransmission was labeled as an area of RPE attenuation or disruption and choroidal hypertransmission with overlying photoreceptor degeneration.[13,16] Reticular pseudodrusen were defined as discrete accumulations of hyper-reflective material above the RPE.[17] The dPED content was classified as homogeneous if it exhibited an internally uniform ground-glass reflectivity.[18]

Quantitative SD-OCT Measurements

SD-OCT raster scans were exported as JPEG and imported into ImageJ software for analysis (National Institutes of Health, Bethesda, MD, USA). The dPED maximum height was measured as the longest distance between the RPE and the BrM. Subfoveal choroidal thickness was determined as the distance between BrM and the sclero-choroidal junction beneath the fovea, with a scale of 1 pixel to 1 micron applied. The dPED area, surface, and volume were calculated using the Cavalieri principle of stereological analysis:[9]

$$\sum_{1}^{k} BrM\ length\ (scan\ n) \times d \quad (1)$$

$$\sum_{1}^{k} RPE\ length\ (scan\ n) \times d \quad (2)$$

$$\sum_{1}^{k} dPED\ Area\ (scan\ n) \times d \quad (3)$$

Taking "d" as the distance between two B-scans (240 µm) and "k" as the identification number of the SD-OCT B-scan. In particular, the dPED area (1) was measured as dPED projection on the BrM; the dPED surface (2) as the length of the RPE above the dPED, and the dPED volume (3) as total area between the RPE and the BrM on each SD-OCT slab (Supplementary Fig. S1).

The surface-to-volume ratio (S/V) was computed by dividing the surface area of the dPED by its volume, and it was expressed in L−1 (inverse length, μm^{-1}).[19] When examining a given volume of an object, the S/V is minimal for a perfect sphere and increases as the object becomes more irregular.

Quantitative BAF Measurements

In eyes that experienced dPED collapse, the area of RPE atrophy was measured on BAF imaging using semi-automatic software RegionFinder. Areas with BAF signal similar to the optic nerve head or retinal blood vessels were measured at each follow-up visit.[20] The margins of RPE atrophy were confirmed using near-infrared imaging co-registered with SD-OCT. No minimum lesion size was set. In eyes where CNV developed after dPED collapse, measurements were performed until the onset of CNV, at which point the follow-up was truncated.

Statistical Analysis

Statistical calculations were performed using the open-source programming language R. Continuous variables were summarized as mean ± standard deviation (SD) or median and interquartile range (IQR), whereas categorical variables were summarized as absolute and relative prevalence.

Three longitudinal outcomes were defined for analysis:

1) The dPED dynamics, including changes in dPED volume and its morphologic features. The McNemar test was applied for qualitative variables, whereas linear models were used for quantitative variables. Discrepancies between eyes with dPED collapse and those without dPED collapse were examined using linear or logistic regression models. The interaction among dPED metrics, time, and covariates was interpreted as the rate of change.
2) Incidence of dPED collapse, was calculated using the Kaplan-Meier survival estimator. Eyes in which the event did not occur were censored at the last visit. A multivariable Cox regression analysis was used for identifying risk factors associated with dPED collapse, including baseline dPED volume as a controlling factor. Hazard ratios (HRs) and confidence intervals (CIs) were provided.
3) The rate of RPE atrophy expansion after dPED collapse, was determined by regressing the square-root transformed RPE atrophy area against time.[20]

Quantitative associations were examined using Pearson correlations for univariable analyses. The impact of dPED characteristics on VA was studied with regression models, with VA values transformed into a continuous LogMAR scale. This analysis included time as a covariate, alongside both quantitative and qualitative factors. The fixed-effect estimate captured the mean effect at the presenting visit. The interaction term between time and group status (dPED collapse versus no dPED collapse) provided insights into the rate of change. Subsequently, pairwise comparisons were conducted among marginal means for different follow-up durations, with adjustments for multiple comparisons.

In the VA analysis, the focus was initially on the follow-up period from baseline to the dPED collapse event, excluding post-collapse data. To scrutinize changes in the rate of vision decline before and after dPED collapse, a linear spline model was applied to the entire dataset, introducing a knot at the median time of dPED collapse. A noticeable shift in slope in this model denoted a substantial alteration in the rate of vision decline. Missing data were handled using the makeX package, which replaced missing observations with the mean from the available data. For dummy categorical variables, the package used the mean proportions for each level. A significance threshold of $P < 0.05$ was set for all statistical analyses.

Results

This longitudinal study included 44 eyes from 34 patients with dPED. The clinical and demographic characteristics of the patients are presented in Table 1.

dPED Characteristics at Baseline

Significant correlations were observed among dPED area, surface, and volume ($P < 0.05$ for all pairs). Furthermore, the dPED area ($r = -0.32$, $P = 0.005$) and dPED surface ($r = -0.28$, $P = 0.07$) showed an inverse correlation with age, suggesting that older patients tended to have smaller dPEDs. The dPED metrics were inversely correlated with the S/V, with the strongest association found between S/V and dPED maximum height ($r = -0.72$, $P < 0.001$; Supplementary Fig. S2). This indicates that taller dPEDs had a smaller surface area than flatter and more irregular dPEDs for a given volume (Fig. 1).

VA at presentation was associated with the dPED area ($P = 0.01$) and dPED surface ($P = 0.01$), but not with the dPED maximum height ($P = 0.3$). Eyes presenting with associated AVL demonstrated poorer VA compared to those without AVL ($P = 0.002$). Similarly, eyes exhibiting RPE hypertransmission showed worse presenting vision ($P = 0.04$; Supplementary Table S2).

Table 1. Baseline Demographic and Clinical Characteristics of Included Patients With Drusenoid Pigment Epithelium Detachment (dPED)

	Overall ($N = 44$)
Age (y)	
Mean (SD)	68 (6.88)
Median [min, max]	70 [56, 80]
Gender	
Male	12 (27%)
Female	32 (73%)
VA (LogMAR)	
Mean (SD)	0.34 (0.31)
Median [min, max]	0.26 [0, 1.30]
dPED area (mm^2)	
Mean (SD)	5.60 (3.46)
Median [min, max]	5.63 [0.46, 14]
dPED surface (mm^2)	
Mean (SD)	6.15 (3.64)
Median [min, max]	6.13 [0.55, 15]
dPED volume (mm^3)	
Mean (SD)	1.34 (1.25)
Median [min, max]	0.79 [0.05, 4.45]
S/V (μm^{-1})	
Mean (SD)	7.20 (4.69)
Median [min, max]	5.97 [2.08, 25]
dPED maximum height (µm)	
Mean (SD)	315 (139)
Median [min, max]	310 [63, 698]
Choroidal thickness (µm)	
Mean (SD)	267 (79)
Median [min, max]	259 [113, 472]
HRF*	
No	14 (32%)
Yes	29 (66%)
Homogeneous content*	
No	16 (36%)
Yes	27 (62%)
Subretinal fluid*	
No	31 (71%)
Yes	12 (27%)
RPE hypertransmission*	
No	28 (64%)
Yes	15 (34%)
AVL*	
No	31 (71%)
Yes	12 (27%)
RPD	
No	32 (74%)
Yes	11 (26%)
Follow-up duration (mo)	59 ± 41

VA, visual acuity; S/V, surface/volume ratio; HRF, hyper-reflective foci; AVL, acquired vitelliform lesions; RPD, reticular pseudodrusen.
* Indicates variables with missing data.

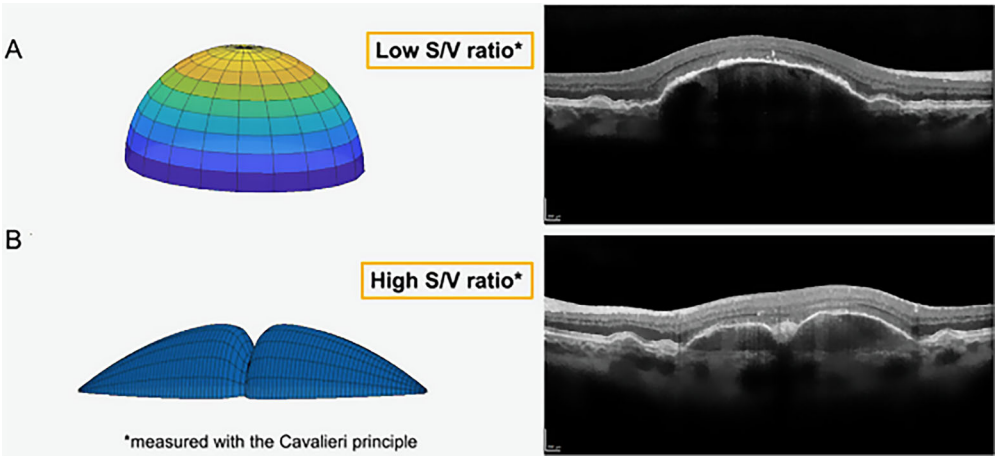

Figure 1. Comparison of graphic modeling and B-scan optical coherence tomography (OCT) images depicting drusenoid pigment epithelial detachment (dPED) with varying surface-to-volume ratios (S/V ratio). (**A**) Graphic modeling and B-scan OCT reveal a regular domed shape dPED with a low S/V ratio, measured using the Cavalieri principle. (**B**) Graphic modeling and B-scan OCT demonstrate an irregular dPED with a high S/V ratio, measured using the Cavalieri principle.

dPED Dynamics and Vision Changes

A total of 29 eyes (66%) experienced dPED collapse over an average follow-up of 58.9 ± 41.3 months (range = 3–139 months; Fig. 2, Supplementary Fig. S3A). The incidence rate of dPED collapse was 22 per 100 eye-years (95% CI = 14 to 32), with a median time from baseline to event of 39 months (95% CI = 25 to 63). Median follow-up period for eyes that did not undergo dPED collapse was 33 months. This duration did not exhibit a significant difference when compared to the median time to the event of eyes that did experience dPED collapse ($P = 0.75$). Subsequently, 28 eyes (64%) developed RPE atrophy after dPED collapse, and 3 eyes (7%) progressed to CNV.

In eyes experiencing dPED collapse, there were noteworthy increases over time in dPED area ($P = 0.03$), dPED surface ($P = 0.02$), and dPED volume ($P = 0.006$; Supplementary Table S3). Conversely, smaller changes were observed in eyes with dPED that did not collapse. Notably, in eyes with dPED collapse, the dPED area, surface, and volume exhibited a more rapid rate of increase (interaction term with time, $P < 0.001$; Supplementary Fig. S4A).

For eyes with dPED collapse, the proportion of eyes with HRF ($P = 0.04$) and RPE hypertransmission ($P = 0.02$) significantly increased, whereas the proportion of eyes with homogeneous dPED content decreased ($P = 0.04$). Conversely, no significant changes were noted in eyes where dPED did not collapse.

Before dPED collapse, there were no significant changes in VA ($P > 0.05$ in both groups), and the two groups had similar rates of visual change ($P = 0.2$). However, eyes with dPED collapse had significantly worse vision since baseline ($P = 0.001$) and experienced significant visual drop at dPED collapse ($P < 0.001$; Fig. 3A). Afterward, VA tended to stabilize.

Risk Factors for dPED Collapse

In a multivariable Cox regression analysis, the presence of RPE hypertransmission (HR = 3.68, 95% CI = 1.52 to 8.92, $P = 0.004$) and HRF (HR = 3.45, 95% CI = 1.20 to 9.97, $P = 0.02$) were identified as the main risk factors for dPED collapse (Table 2). A higher S/V was a significant protective factor for dPED collapse (HR = 0.78, 95% CI = 0.63 to 0.97, $P = 0.03$; see Supplementary Fig. S3B–D).

Rate of RPE Atrophy Enlargement after dPED Collapse

The square-root rate of RPE atrophy growth after dPED collapse was determined as 0.42 ± 0.26 mm/year (see Supplementary Fig. S4B). RPE atrophy enlargement occurred at a faster rate in eyes with higher dPED area ($r = 0.60$, $P < 0.001$), surface ($r = 0.59$, $P < 0.001$), and volume ($r = 0.57$, $P = 0.005$). A faster rate of RPE atrophy enlargement was associated with a faster rate of dPED volume increase ($r = 0.47$, $P = 0.02$) and worse VA over time ($P = 0.02$; see Fig. 3B).

Discussion

The present study aimed to investigate the clinical characteristics of patients with dPED, focusing on the rate of dPED growth, the incidence of dPED collapse, and their impact on VA. Additionally, we explored the rate of RPE atrophy enlargement after dPED collapse, providing insights into the factors associated with progression to late AMD in eyes with high-risk iAMD.

The Age-Related Eye Disease Study (AREDS) hypothesized that patients with dPED may represent a distinct subset of individuals with iAMD, characterized by younger age, worse vision, and a higher risk of progressing to late AMD compared to eyes with only drusen or pigmentary changes.[2] The advancements in SD-OCT resolution have allowed for the identification of dPED characteristics associated with both visual and anatomic prognosis, such as dPED volume, area, and maximum height.[3] In our study, we found a significant association among VA and dPED area, surface, and dPED volume but not with dPED maximum height, indicating that the horizontal extent of the dPED had a greater impact on VA than its vertical extent. Further studies utilizing high-density SD-OCT macular maps and using techniques

Investigative Ophthalmology & Visual Science

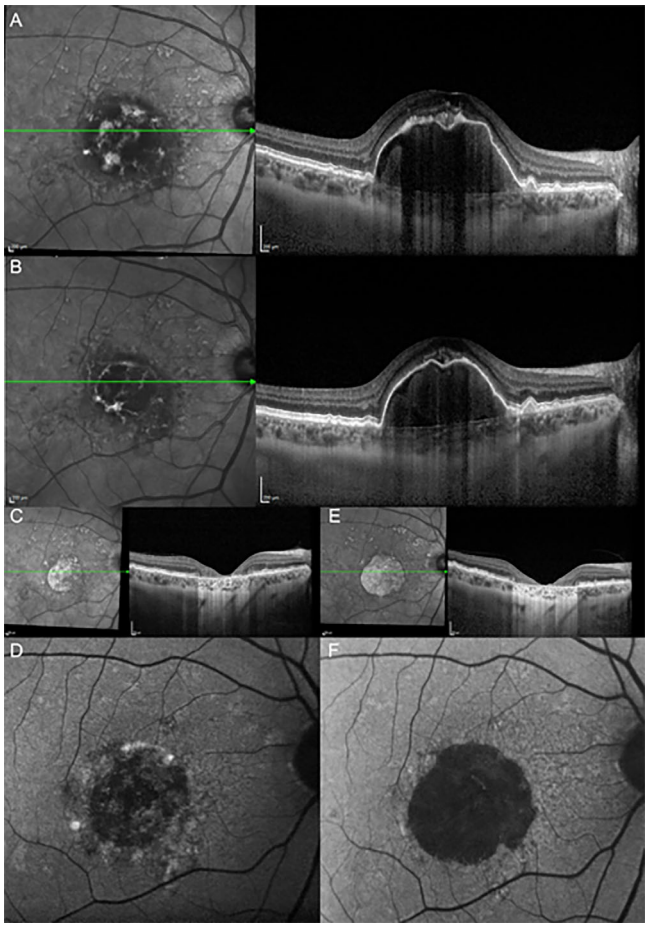

Figure 2. Longitudinal changes in a patient with drusenoid pigment epithelium detachment (dPED) and subsequent retinal pigment epithelium (RPE) atrophy expansion after dPED collapse. (**A**). Combined fundus infrared reflectance (IR) and structural optical coherence tomography (OCT) display the presence of a dPED with subretinal hyper-reflective vitelliform material above it. (**B**) Combined fundus IR and structural OCT exhibit the disappearance of subretinal hyperreflective vitelliform material above the dPED. (**C**) Combined fundus IR and structural OCT demonstrate the collapse of the dPED, accompanied by RPE and outer retina atrophy. (**D**) Combined fundus IR and structural OCT highlight the progression of RPE and outer retina atrophy following dPED collapse. (**E**) Blue-light fundus autofluorescence (BAF) reveals a circular area of hypo-autofluorescence, corresponding to RPE atrophy after dPED collapse. Surrounding the circular hypo-autofluorescent area, irregular hyper-autofluorescence can be observed. (**F**) BAF demonstrates a larger area of hypo-autofluorescence, indicating RPE atrophy progression.

such as the Cavalieri method are required to validate our observations.

The presence of AVL and RPE hypertransmission was associated with worse presenting vision. AVL results from the accumulation of lipofuscin, melanolipofuscin, melanosomes, and outer segment debris in the subretinal space and has been regarded as a nonspecific sign of RPE distress.[21] Similarly, appearance of AVL was reported to precede the dPED collapse, but authors did not investigate VA changes.[6] On the other hand, the presence and extent of RPE atrophy have been shown to correlate linearly with visual function.[22] These associations underscore the clinical significance of morphological dPED characteristics as prognostic indicators in patients with iAMD. We observed an inverse correlation between age and dPED area and surface, suggesting that older patients tended to present with smaller dPEDs. This association between age and dPED size implies potential age-related mechanisms in the pathogenesis of dPED, possibly involving a progressively slower rate of drusenoid material accumulation over time. Conversely, it might indicate that patients with larger dPEDs had already experienced collapse at a younger age. In fact, the detection of dPED is relatively rare after 80 years of age.[2,4] Interestingly, older age was also associated with a slower rate of dPED volume change, reinforcing the hypothesis that drusenoid material deposition may vary with time.

Regarding dPED collapse, a substantial proportion of eyes (66%) experienced this event during the follow-up period. The estimated incidence rate of dPED collapse was 22 per 100 eye-years, consistent with recent natural history studies.[4] In the assessment and comparison of dPED collapse incidence rate, it is of utmost importance to have similar follow-up periods and similar methodology, which otherwise could bring out major discrepancies. Eyes that experienced dPED collapse exhibited worse baseline VA and demonstrated a significant VA decline when the event occurred, underscoring the critical impact of this event on vision. Our findings also revealed that, in the later stages, when more than half of the cohort of eyes experienced dPED collapse, the rate of visual decline stabilized, highlighting the clinical implications of dPED collapse in determining the long-term prognosis of patients with iAMD.[7,9]

Our multivariable analysis identified the presence of HRF as a significant risk factor for dPED collapse, consistent with a previous study, suggesting that RPE disintegration is a critical factor heralding dPED re-absorption and RPE atrophy formation.[18] Additionally, the presence of RPE hypertransmission increased the risk of dPED collapse. A recent study using en face OCT images demonstrated that hypertransmission RPE defects could serve as a standalone precursor sign for future geographic atrophy formation.[23] Our results align with the hypothesis that RPE hypertransmission could represent a point of no return for RPE disruption and indicate near-term disease progression.

Until now, studies have focused on the volume of PEDs and volume growth rate, without taking into account their shape.[3,6,10] In this study, we introduced the concept of S/V as a significant protective factor against dPED collapse. S/V represents the amount of surface area per unit volume. For a given volume, a sphere has the smallest surface area and the smallest S/V, whereas objects with angled or irregular shapes have larger surface areas.[19] The concept of S/V is widely used in science to explain processes, such as oxygen or particle diffusion across cell membranes and thermal conduction.[24] It can also be applied to biophysics, where a wider surface and larger base of a 3D object provide a broader support area, lowers the center of gravity, and increases the moment of force required to topple it, resulting in greater stability.[25] Our study found that higher S/V values were associated with a slower rate of dPED volume change, suggesting that taller and straighter dPED lesions tended to grow faster than flatter irregular lesions. Presumably, this is connected to a greater separation distance from the underlying choroid, which is the main source of nourishment for the RPE.[26]

Finally, we investigated the expansion rate of RPE atrophy, a common sequela following drusen re-absorption.[2] Although previous studies focused on the risk of advanced

Investigative Ophthalmology & Visual Science

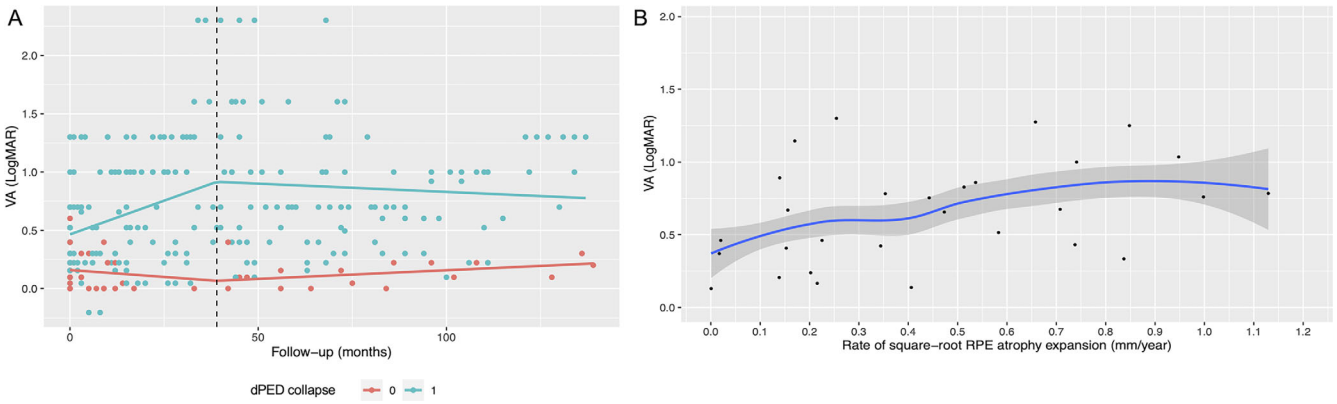

Figure 3. Longitudinal changes of visual acuity (VA) based on drusenoid pigment epithelium detachment (dPED) collapse and the rate of retinal pigment epithelium (RPE) atrophy expansion. (**A**) Line plot displays the longitudinal changes in VA for eyes with dPED, stratified based on whether they experienced dPED collapse or not. A vertical line indicates 39 months (the median time of dPED collapse). (**B**) Scatter plot demonstrates the association between VA and the rate of square-root of RPE atrophy expansion.

Table 2. Risk Factors for Drusenoid Pigment Epithelium (dPED) Collapse Over Follow-Up on Univariable Analysis

	Univariable		Multivariable	
	HR (95% CI)	***P* Value**	**HR (95% CI)**	***P* Value**
Age (for 1-y)	0.98 (0.92–1.04)	0.4		
Gender (ref: male)	1.51 (0.61–3.72)	0.4		
Baseline VA (for 1 LogMAR)	1.60 (0.66–3.88)	0.3		
dPED area (for 1 mm^2)	1.12 (1.00–1.35)	0.04*		
dPED surface (for 1 mm^2)	1.12 (1.01–1.25)	0.04*		
dPED volume (for 1 mm^3)	1.40 (1.02–1.93)	0.04*		
Rate of dPED volume increase (cube root, for 1 mm/mo)	1.15 (1.00–1.25)	0.6		
S/V (for 1 μm^{-1})	0.88 (0.80–0.98)	0.02*	0.78 (0.63–0.97)	0.03
dPED maximum height (for 1 µm)	1.00 (0.99–1.004)	0.5		
SCT (for 1 µm)	1.00 (0.99–1.01)	0.9		
HRF (ref: no)	2.57 (1.47–2.03)	0.04*	3.45 (1.20–9.97)	0.02
Homogeneous content (ref: no)	0.53 (0.25–1.13)	0.09		
Subretinal fluid (ref: no)	1.04 (0.39–2.83)	0.9		
RPE hypertransmission (ref: no)	3.51 (1.59–7.73)	0.002*	3.68 (1.52–8.92)	0.004
AVL (ref: no)	1.14 (0.52–2.48)	0.9		

VA, visual acuity; S/V, surface/volume ratio; SCT, subfoveal choroidal thickness; HRF, hyperreflective foci; AVL, acquired vitelliform lesions. Hazard ratio (HR) and 95% confidence interval (CI) are reported for each variable.
* $P < 0.05$.

AMD progression, they did not explore the rate of RPE atrophy expansion and potentially structural risk factors associated with the dPED.[2,10] Investigating the expansion rate of RPE atrophy helps identify patients at higher risk of blindness from late AMD, similar to previous studies focused on geographic atrophy progression.[27] We observed that the rate of RPE expansion was relatively higher than previously reported.[27] This discrepancy could be attributed to the inclusion of only patients with larger dPED, suggesting that these patients may have started with larger lesions. Conversely, our study may provide evidence of a higher risk of RPE atrophy enlargement in patients with dPED. Recent research identified dPED volume as an independent risk factor for transitioning to late AMD.[28] We found a significant association between RPE atrophy enlargement and the rate of dPED volume change, indicating that faster dPED growth was also a predictor of faster RPE atrophy enlargement after collapse. A faster rate of RPE atrophy enlargement was also associated with worse VA, emphasizing the clinical relevance of RPE atrophy and its progression in terms of visual impairment and the need for early treatment in fast progressors.

Overall, our study provides insights into the clinical characteristics, dynamics, and prognostic factors of dPED. The correlation among dPED morphological parameters, the association of age with dPED size, and the impact of dPED collapse on VA highlight the complex nature of dPED. The identification of risk factors for dPED collapse, such as RPE hypertransmission and HRF, and the protective effect of a higher S/V ratio can aid in risk stratification. Furthermore, the evidence of RPE atrophy enlargement after dPED collapse underscores the importance of monitoring and managing this secondary manifestation.

In this study, we leveraged all available follow-up data without imposing specific time intervals or predefined end points. To mitigate potential biases arising from variations in follow-up durations and ensure the robustness of our findings, we used Cox regression analysis. This statistical approach allowed us to account for differences in follow-up times and potential heterogeneity among the study partici-

pants. Despite these valuable strengths, our study has limitations. Additionally, multivariable Cox regression analysis included baseline dPED volume to mitigate potential selection bias, because patients with larger drusen and worse vision are more prone to be referred to the study center. The retrospective design and relatively small sample size may limit the generalizability of the results. The lack of additional multimodal imaging modalities, such as OCT angiography, or specific imaging reconstruction techniques, such as en face imaging, may have prevented additional information on dPED natural history. The high collinearity between dPED measures precluded from the use of multiple variable adjustments in regression analyses. Finally, the focus on dPED characteristics when assessing factors associated with RPE atrophy enlargement may introduce potential biases. Future studies with larger sample sizes, prospective designs, and more comprehensive evaluations are warranted to corroborate our findings.

Acknowledgments

Funding/Support: This research received no specific grant from funding agencies in the public, commercial, or not-for-profit sectors.

Contributorship Statements: All the authors contributed to the conception or design of the work, the acquisition, analysis, and interpretation of data, drafting of the work, revising it critically for intellectual content. Each of the coauthors has seen and agrees with the way his or her name is listed.

A.C. Morelli, is a PhD Student in Space Engineering, for the graphic modeling of drusenoid pigment epithelium detachment.

Disclosure: **M. Menean**, None; **A. Apuzzo**, None; **U. Introini**, None; **F. Bandello**, AbbVie (C), Alimera (C), Bayer Shering-Pharma (Berlin, Germany) (C), Boehringer-Ingelheim (C), Hoffmann-La-Roche (Basel, Switzerland) (C), Novartis (Basel, Switzerland) (C), Oxurion NV (C), Ntc Pharma (C), Sifi (C); **M.V. Cicinelli**, None

References

1. Hartnett ME, Weiter JJ, Garsd A, Jalkh AE. Classification of retinal pigment epithelial detachments associated with drusen. *Graefes Arch Clin Exp Ophthalmol*. 1992;230(1):11–19.
2. Cukras C, Agron E, Klein ML, et al. Natural history of drusenoid pigment epithelial detachment in age-related macular degeneration: age-related eye disease study report no. 28. *Ophthalmology*. 2010;117(3):489–499.
3. Tvenning AO, Krohn J, Forsaa V, et al. Drusenoid pigment epithelial detachment volume is associated with a decrease in best-corrected visual acuity and central retinal thickness: the Norwegian Pigment Epithelial Detachment Study (NORPED) report no. 1. *Acta Ophthalmol*. 2020;98(7):701–708.
4. Yu JJ, Agron E, Clemons TE, et al. Natural history of drusenoid pigment epithelial detachment associated with age-related macular degeneration: age-related eye disease study 2 report no. 17. *Ophthalmology*. 2019;126(2):261–273.
5. Schlanitz FG, Baumann B, Kundi M, et al. Drusen volume development over time and its relevance to the course of age-related macular degeneration. *Br J Ophthalmol*. 2017;101(2):198–203.
6. Balaratnasingam C, Yannuzzi LA, Curcio CA, et al. Associations between retinal pigment epithelium and drusen volume changes during the lifecycle of large drusenoid pigment epithelial detachments. *Invest Ophthalmol Vis Sci*. 2016;57(13):5479–5489.
7. Thavikulwat AT, De Silva T, Agron E, et al. Multimodal assessments of drusenoid pigment epithelial detachments in the age-related eye disease study 2 ancillary spectral-domain optical coherence tomography study cohort. *Retina*. 2022;42(5):842–851.
8. Hirabayashi K, Yu HJ, Wakatsuki Y, et al. OCT risk factors for development of atrophy in eyes with intermediate age-related macular degeneration. *Ophthalmol Retina*. 2023;7(3):253–260.
9. Balaratnasingam C, Hoang QV, Inoue M, et al. Clinical characteristics, choroidal neovascularization, and predictors of visual outcomes in acquired vitelliform lesions. *Am J Ophthalmol*. 2016;172:28–38.
10. Shijo T, Sakurada Y, Tanaka K, et al. Incidence and risk of advanced age-related macular degeneration in eyes with drusenoid pigment epithelial detachment. *Sci Rep*. 2022;12(1):4715.
11. Liao DS, Grossi FV, El Mehdi D, et al. Complement C3 inhibitor pegcetacoplan for geographic atrophy secondary to age-related macular degeneration: a randomized phase 2 trial. *Ophthalmology*. 2020;127(2):186–195.
12. Jaffe GJ, Westby K, Csaky KG, et al. C5 inhibitor avacincaptad pegol for geographic atrophy due to age-related macular degeneration: a randomized pivotal phase 2/3 trial. *Ophthalmology*. 2021;128(4):576–586.
13. Jaffe GJ, Chakravarthy U, Freund KB, et al. Imaging features associated with progression to geographic atrophy in age-related macular degeneration: classification of atrophy meeting report 5. *Ophthalmol Retina*. 2021;5(9):855–867.
14. Hilely A, Au A, Freund KB, et al. Non-neovascular age-related macular degeneration with subretinal fluid. *Br J Ophthalmol*. 2021;105(10):1415–1420.
15. Koo TK, Li MY. A guideline of selecting and reporting intraclass correlation coefficients for reliability research. *J Chiropr Med*. 2016;15(2):155–163.
16. Sadda SR, Guymer R, Holz FG, et al. Consensus definition for atrophy associated with age-related macular degeneration on OCT: classification of atrophy report 3. *Ophthalmology*. 2018;125(4):537–548.
17. Rabiolo A, Sacconi R, Cicinelli MV, et al. Spotlight on reticular pseudodrusen. *Clin Ophthalmol*. 2017;11:1707–1718.
18. Ouyang Y, Heussen FM, Hariri A, et al. Optical coherence tomography-based observation of the natural history of drusenoid lesion in eyes with dry age-related macular degeneration. *Ophthalmology*. 2013;120(12):2656–2665.
19. Adam J. What's your sphericity index? Rationalizing surface area and volume. *Virginia Mathematics Teacher*. 2020;46(2):48–53, http://www.vctm.org/VOL-462.
20. Feuer WJ, Yehoshua Z, Gregori G, et al. Square root transformation of geographic atrophy area measurements to eliminate dependence of growth rates on baseline lesion measurements: a reanalysis of age-related eye disease study report no. 26. *JAMA Ophthalmol*. 2013;131(1):110–111.
21. Iovino C, Ramtohul P, Au A, et al. Vitelliform maculopathy: diverse etiologies originating from one common pathway. *Surv Ophthalmol*. 2023;68(3):361–379.
22. Savastano MC, Falsini B, Ferrara S, et al. Subretinal Pigment Epithelium Illumination Combined with focal electroretinogram and visual acuity for early diagnosis and prognosis of non-exudative age-related macular degeneration: new insights for personalized medicine. *Transl Vis Sci Technol*. 2022;11(1):35.
23. Shi Y, Yang J, Feuer W, et al. Persistent hypertransmission defects on en face OCT imaging as a stand-alone precursor for the future formation of geographic atrophy. *Ophthalmol Retina*. 2021;5(12):1214–1225.

24. Planinšič G, Vollmer M. The surface-to-volume ratio in thermal physics: from cheese cube physics to animal metabolism. *Eur J Physics*. 2008;29(2):369–384.
25. Serway RA. *Physics for scientists & engineers with modern physics*. Second edition. Philadelphia, PA: Saunders College Publications; 1986, c1983. 1986.
26. Au A, Santina A, Abraham N, et al. Relationship between drusen height and OCT biomarkers of atrophy in non-neovascular AMD. *Invest Ophthalmol Vis Sci*. 2022; 63(11):24.
27. Fleckenstein M, Mitchell P, Freund KB, et al. The progression of geographic atrophy secondary to age-related macular degeneration. *Ophthalmology*. 2018;125(3):369–390.
28. Abdelfattah NS, Zhang H, Boyer DS, et al. Drusen volume as a predictor of disease progression in patients with late age-related macular degeneration in the fellow eye. *Invest Ophthalmol Vis Sci*. 2016;57(4):1839–1846.

Investigative Ophthalmology & Visual Science